ELSEVIER

Journal of Experimental Marine Biology and Ecology
188 (1995) 1–28

JOURNAL OF EXPERIMENTAL MARINE BIOLOGY AND ECOLOGY

Patterns of macromolecular synthesis by natural phytoplankton assemblages under changing upwelling regimes: in situ observations and microcosm experiments

Emilio Marañón [a,*], Emilio Fernández [b], Ricardo Anadón [a]

[a] *Departamento de Biología de Organismos y Sistemas, Unidad de Ecología, Universidad de Oviedo, E-33005 Oviedo, Spain*

[b] *Instituto de Investigacions Mariñas (CSIC), Eduardo Cabello, 6, E-36208 Vigo, Spain*

Received 3 June 1994; revision received 19 October 1994; accepted 1 November 1994

Abstract

A coastal station located in the southern Bay of Biscay was sampled on six occasions between 12 July and 10 September 1991. The vertical distribution of the patterns of photosynthetic carbon incorporation into proteins, polysaccharides, lipids and low molecular weight metabolites, as well as the biochemical composition of particulate matter were determined on each cruise. In addition, the same variables were monitored during microcosm experiments in which sub-surface phytoplankton assemblages were incubated under different rates of increasing irradiance simulating differences in upwelling intensity. During the first three experiments, phytoplankton cells did not show any growth response to the simulated upwelling conditions. When phytoplankton growth was slow or absent and nutrients were still available, the relative synthesis of proteins was high, suggesting that phytoplankton cells tended to maintain the synthesis of proteins rather than storage products under adverse growth-limiting conditions. Sub-surface phytoplankton assemblages had the potential for growth in response to upwelling. Several diatom blooms developed during the last two experiments showing enhanced levels of protein and polysaccharide specific synthesis rates (SSR) and a marked increase in the protein to carbohydrate (P:C) compositional ratio. Parallel sea-truth observations carried out during an upwelling pulse indicated that phytoplankton assemblages under natural conditions underwent similar physiological changes to those found in the experimental microcosms under simulated upwelling. In general, the most remarkable increases in chlorophyll *a* (Chl *a*) concentration and macromolecular SSR took place in those microcosms showing higher rates of increasing irradiance. Variations in the patterns of photosynthate partitioning and the P:C ratio were also related to the intensity of the advective process. These results emphasize the importance of the fine variability of the physical field in modulating the physiological responses of phytoplankton to upwelling.

* Corresponding author.

SSDI 0022-0981(94)00177-4

Keywords: Biochemical composition; ^{14}C-incorporation pattern; Irradiance change; Phytoplankton; Upwelling

1. Introduction

In coastal upwelling areas, longshore winds induce horizontal divergences displacing surface waters offshore, thus giving rise to advection of sub-surface waters to surface layers. In such hydrographic scenarios, sub-surface phytoplankton populations experience simultaneously high irradiance and nutrient-rich conditions whilst they are transported upwards during the upwelling event. When advection of deep water ceases, phytoplankton cells are exposed to decreasing irradiance as they eventually sink down to deeper waters. As a consequence of these dynamic processes, phytoplankton populations undergo a series of physiological changes at the cellular level tending to adjust their nitrogen and carbon metabolism to the new physical and chemical environment imposed by upwelling.

In this context, the study of the ^{14}C partitioning into different cellular constituents has been shown to be a useful tool in assessing changes in physiological state and growth rate of phytoplankton occurring as a response to a changing environment, both in cultures (e.g. Morris et al., 1974; Konopka & Schnur, 1981; Hitchcock, 1983; Rivkin, 1989) and natural populations (e.g. Morris & Skea, 1978; Morris et al., 1981; Fernández et al., 1992). As stated by Morris (1981), the study of the patterns of photosynthate partitioning is an autotroph-specific approach which reveals the inmediate physiological responses of the algae to their growth conditions on relatively short time scales. However, cellular biochemical composition represents the integration of those responses over longer time periods. The combination of these two approaches in the same investigation allows the study of phytoplankton ecophysiology over two different time scales. Moreover, the determination of photosynthetic parameters derived from photosynthesis-irradiance curves potentially provide further insight into the physiological state of phytoplankton, as they are indicators of the adaptation of phytoplankton to different light regimes.

Knowledge of changes in carbon metabolism and biochemical composition experienced by natural phytoplankton populations during advective processes is scarce. High percentages of ^{14}C incorporation into proteins have been reported for a coastal upwelling area, although the lowest values of relative protein synthesis were found in waters associated with the upwelling center (Priscu & Priscu, 1984). Relative carbon incorporation into proteins was shown to be dependent on the turbulent regime to which algae were exposed, highest values being found when physical stability increased (Barlow, 1984). As far as the biochemical composition of particulate matter is concerned, decreases in the protein to carbohydrate ratio have been noticed during the declining phase of a phytoplankton bloom after an upwelling event (Barlow, 1980).

Variations in photosynthetic carbon metabolism and biochemical composition in multi-specific natural populations are difficult to interpret, because the controlling factors are highly variable and it becomes complex to differentiate between within-species

physiological changes and variations in species composition. The use of experimental enclosures (meso- and microcosms) overcomes some of these problems, enabling the study of the same phytoplankton assemblage under controlled conditions. In this regard, several studies undertaken with phytoplankton populations growing under simulated upwelling conditions have contributed to a better knowledge of the physiological changes experienced by phytoplankton cells when exposed to increased light and nutrient levels. These studies show that the exposure of sub-surface phytoplankton populations to upper water column conditions often leads to increases in growth rate and to the development of diatom blooms (Ishizaka et al., 1983; Pitcher et al., 1993). Enhanced nitrate uptake rates and nitrate reductase activity have been also found under simulated upwelling conditions (Jason Smith et al., 1992). However, none of these experimental studies dealt with the effect of different intensities of advection upon photosynthetic carbon metabolism and biochemical composition of phytoplankton populations.

In this study, changes in photosynthetic parameters, ^{14}C-labelling patterns of macromolecules and the biochemical composition of particulate matter were investigated during field surveys, and in a series of experiments with microcosms throughout the summer of 1991. Since the intensity of upwelling events is highly variable, and given that microalgae undergo complex physiological adjustments during acclimation to new irradiance and nutrient regimes, it may be hypothesized that the rate at which environmental changes take place must be important in controlling the physiological state of phytoplankton cells.

The main objectives of this study were: (1) to determine the influence of upwelling on ^{14}C-incorporation patterns and biochemical composition of natural phytoplankton assemblages, (2) to find out whether sub-surface phytoplankton populations have the potential to adjust their photosynthetic metabolism to the rapid environmental changes imposed by upwelling processes, and (3) to ascertain the effect of different regimes of increasing irradiance, simulating different upwelling and downwelling velocities, on growth rates and the differential synthesis of macromolecules in natural phytoplankton assemblages.

2. Methods

2.1. Field study

Sampling was conducted at a coastal station (43° 36′ N, 6° 08′ W; depth 60 m) located in the Central Cantabrian Sea (southern Bay of Biscay). Six cruises were carried out between 12 July and 10 September 1991. On each cruise, water samples were drawn from 0, 10, 20 30 and 40 m using Niskin bottles equipped with reversing thermometers. The vertical distribution of irradiance (400–700 nm) was measured with a Li-Cor 4π underwater sensor. Duplicate 6 ml polyethylene tubes were filled with water from the Niskin bottles and stored at 20 °C until further analysis of nitrate and silicate following the methods described in Grasshoff et al. (1983).

Chlorophyll *a* concentration was determined in duplicate after filtration of 100 ml

water samples through Whatman GF/F glass fibre filters, which were inmediately frozen. Chlorophyll *a* concentration was measured fluorometrically after grinding and extraction of the filters in 90% acetone for 10 min at 4 °C. Phytoplankton samples were preserved in Lugol's iodine solution and counted with an inverted microscope. Duplicate water samples for protein and carbohydrate analysis were filtered through preashed Whatman GF/F fibre filters and stored at −20 °C. Protein and carbohydrate concentrations were determined following the methods of Lowry et al. (1951) and Dubois et al. (1956), respectively, using glucose and bovine serum albumine as standards.

In order to determine the distribution patterns of ^{14}C incorporation into the end-products of photosynthesis, triplicate 1-l water samples were taken from the Niskin bottles and kept at 15 ± 1 °C in darkness, and transported to the laboratory within 2–3 h. Incubations were carried out in a controlled temperature room at 15 ± 0.5 °C. Two 70 ml polycarbonate bottles were filled from each 1-l bottle and then inoculated with 370 kBq (10 μCi) of $NaH^{14}CO3$ (Dupont NEN Products; specific activity, 2.1 GBq·mmol^{-1}). One of the samples was incubated for 10 h under continuous light, whereas the other one was incubated for 24 h under a 10 L:14 D photoperiod in order to assess dark reallocation of photosynthate. Bottles were illuminated with cold white light from "Sylvania" fluorescent tubes. Samples were incubated at aproximately their original irradiance level, assuming a surface irradiance value of 300 $\mu E \cdot m^{-2} \cdot s^{-1}$. This irradiance level was typical of the upper mixed layer (0–15 m depth) throughout the study. At the end of the incubations, samples were filtered through Whatman GF/F filters under a low vacuum pressure (< 100 mm Hg). The filters were then placed in polyethylene vials with 1 ml methanol/acetic acid mixture (99:1 v/v), and stored frozen (−20 °C) until further analysis.

Incorporation of ^{14}C into different cellular constituents was determined following a procedure modified from Li et al. (1980) and Lohrenz & Taylor (1987). This procedure separates cell material into 4 fractions: methanol/water-soluble compounds (low molecular weight metabolites, LMWM), chloroform-soluble compounds (lipids), hot trichloroacetic acid (TCA)-soluble compounds (polysaccharides and nucleic acids) and hot TCA-insoluble compounds (proteins). This method does not take into account the production of dissolved organic matter during photosynthesis. However, the amount of photosynthetically fixed ^{14}C released as soluble material was monitored during this study, using the acidification and bubbling method described in Mague et al. (1980). In all cases, the contribution of this soluble fraction to the total particulate carbon production was less than 5%. Therefore, it is unlikely that the production of dissolved organic matter would exert a signicant influence on the patterns of ^{14}C allocation during the present study.

The analytical routine first involved vortex-mixing of the filter with 3.0 ml of chloroform and 1.5 ml of the methanol/acetic acid mixture. The filter was kept at 4 °C for 10 min and the resulting suspension transferred to a graduated tube. The filter was vortex-mixed again with chloroform and methanol/acetic acid mixture. After keeping the filter at 4 °C for another 10 min, a second suspension was obtained and transferred to a second graduated tube. 1 ml of distilled water was added to both suspensions and then they were vortexed, centrifuged for 10 min at 4000 rpm and 1 ml aliquots taken

from each phase. The aliquots were immediately transferred to a vial, in the case of the upper phase containing LMWM, or allowed to air dry, in the case of the chloroform phase, before 4 ml of scintillation cocktail (INSTA-GEL) were added. The carbon incorporation into lipids and LMWM was calculated as the sum of the ^{14}C activity in the aliquots from both extractions.

The filter was then transferred to a glass tissue-homogenizer and ground in 1.5 ml 5% (w/v) trichloroacetic acid (TCA). After rinsing the filter with 3 ml of TCA, the suspension was heated at 95 °C for 20 min and subsequently centrifuged at 4000 rpm for 20 min. The supernatant was transferred to another tube, the pellet resuspended with TCA and extracted again at 95 °C for 10 min. After centrifugation, the supernatant was added again to the supernantant from the previous extraction, and the residual pellet rinsed sequentially with 0.5 ml 0.1 N NaOH, 1 ml distilled water and 0.75 ml 1.0 M Tris (pH: 7.0). Finally, 1 ml-aliquots from both the TCA and the residual fractions were transferred to 20 ml-scintilllation vials and 10 ml of scintillation cocktail added. CPM were corrected for quenching using an internal standard. Daily primary production was calculated as the sum of the ^{14}C incorporated into each fraction. The sum of the ^{14}C activity in the 4 fractions accounted for 90–104% of the total activity as measured in parallel non-fractionated samples.

Daily specific synthesis rates (SSR) for proteins and polysaccharides were calculated according to the equation:

$$SSR = C_i/C_p$$

where C_i is the amount of carbon incorporated into a given metabolic fraction during a 24-h incubation and C_p is the carbon content of the biochemical pool. Carbon content was calculated as 53% of total weight for proteins, taking into account the average composition of microalgae proteins (Laws, 1991), and 40% of total weight for carbohydrates, as derived from the carbon composition of the standard (glucose). SSR values may be underestimated if a significant amount of non-algae material were present in the samples. The relative contribution of this material was evaluated by calculating the relationship between chlorophyll *a* (Chl *a*) concentration (Chl *a*) and protein-*N* concentration (Pro-*N*) for the whole set of data collected in this study. This relationship showed a significant fit to the linear function

$$Pro\text{-}N = 0.260 + 0.281 * \text{Chl } a \ (r^2 = 0.75, n = 140, p < 0.001)$$

The low *Y*-intercept in the equation indicated a small significance of non-phytoplankton material. In addition, the average Chl *a*/Pro-*N* ratio was 2.56 ± 0.17, close to the value obtained by Dortch & Packard (1989) (2.88 ± 0.09) in natural samples of very high phytoplankton content.

2.2. Laboratory experiments

A series of laboratory experiments was conducted in parallel to the in situ studies described above. On each cruise, twelve 12-l acid-washed polycarbonate bottles were filled with pre-screened (200 μm mesh size) seawater and kept at 15 ± 1 °C in darkness until arrival at the laboratory 2–3 h later. Seawater was taken with a Van Dorhn bottle either from the thermocline (20–30 m depth), when the water column was stratified, or

from 10 m depth during upwelling phases (see Fig. 1). Each bottle was filled with water from a different bottle cast to assure independence between replicates. Incubations were carried out at constant temperature (15 ± 0.5 °C) under a 10 L:14 D photoperiod. Lights were turned on at 0900 and turned off at 1900. Bottles were placed inside an incubator equipped with rollers which rotated at ≈ 6 rpm, to prevent sedimentation of the cells. Except for treatment A in Exp. 4, nutrients were added to all bottles at the start of the incubation, providing an increase in nutrient concentration of about 5 μM nitrate, 5 μM silicate and 0.5 μM phosphate, with the aim to examine exclusively the effect of irradiance on photosynthetic carbon metabolism and biochemical composition of the cells.

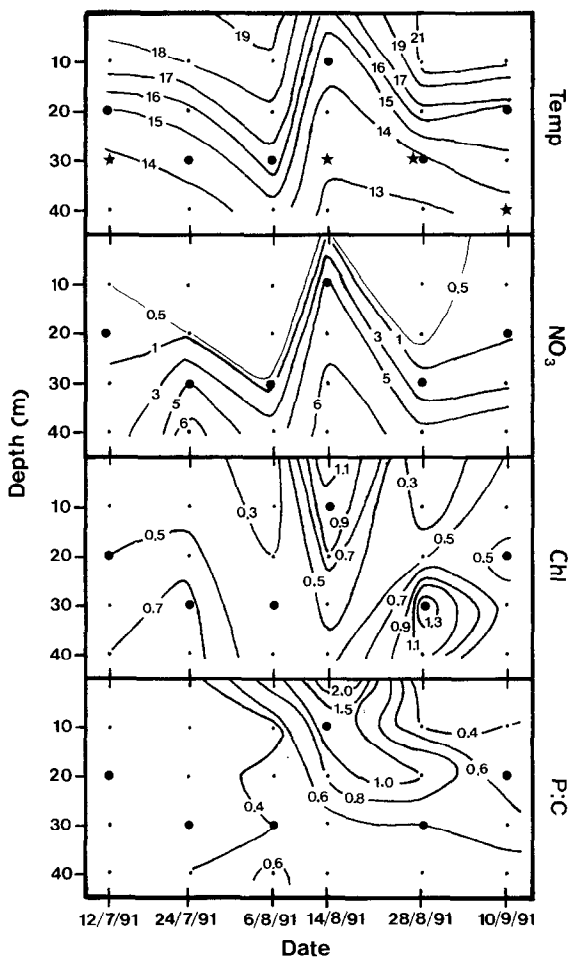

Fig. 1. Vertical distribution of temperature (Temp; °C), nitrate concentration (NO_3; μmol·l^{-1}), chlorophyll *a* concentration (Chl; μg·l^{-1}) and the protein-C:carbohydrate-C ratio (P:C) of the particulate matter at the sampling station throughout the study period. Larger dots indicate depths from where water for the experiments was taken. Stars indicate the depth where irradiance was $\approx 10\%$ I_o.

Four treatments were designed in triplicate (Table 1). In Exps. 1, 2, 3, 5 and 6, treatments B, C and D ("upwelling" treatments) represented three velocities of increasing irradiance, which simulated three different speeds of upward water motion during an upwelling event. The upward velocities estimated for treatments B and C (see Table 1) were within the range of values calculated in natural coastal upwelling situations (Figueiras et al., 1994). Treatment A ("control") represented the maintenance of the samples at their original irradiance level (5–10% I_o). The time zero irradiance (30 $\mu E \cdot m^{-2} \cdot s^{-1}$) used at the start of Exps. 1, 2, 3, 5, and 6 was typically found at the sampling station between 25 and 40 m depth throughout the study. In Exp. 4, treatments C and D simulated two velocities of decreasing irradiance during a downwelling event, whereas treatments A and B corresponded to the maintenance of the cells in the upper layer, without (treatment A) and with (treatment B) addition of nutrients. Irradiance at the beginning of this experiment was 300 $\mu E \cdot m^{-2} \cdot s^{-1}$.

Water samples were taken from the bottles during the experiments in order to assess changes in the same variables monitored during the field cruises. Chlorophyll *a* concentration was measured on a daily basis. Nitrate and silicate concentration, the biochemical composition of particulate material (proteins and carbohydrates), the taxonomic composition of microplankton, and the patterns of ^{14}C-labelling were determined at the beginning, the middle and the end of the experiments. A handling mistake was made with the scintillation vials corresponding to the lipid and LMWM fractions from

Table 1
Irradiance levels ($\mu E \cdot m^{-2} \cdot s^{-1}$) at which the phytoplankton populations were incubated in the different experiments and treatments

Day	Exps. 1[a], 2[a], 3[b], 5[a] and 6[c]				Exp. 4[a]			
	A	B	C	D	A[d]	B	C	D
0	30	30	30	30	300	300	300	300
1	30	50	100	300	300	300	250	150
2	30	100	150	300	300	300	200	100
3	30	150	200	300	300	300	150	50
4	30	200	300	300	300	300	100	30
5	30	250	300	300	300	300	50	30
6	30	300	300	300	300	300	30	30
7	30	300	300	300	300	300	30	30
8	30	300	300	300	–	–	–	–
9	30	300	300	300	–	–	–	–
Stimulated water velocity ($m \cdot day^{-1}$)	0	6	8	30	0	0	6	9

Simulated upwelling and downwelling velocities are shown. These velocities were estimated from the irradiance profiles recorded at the field station during the study. A, B, C and D denote the different treatments.
[a] Exps. 1, 2, 4 and 5 lasted 7 days.
[b] Exp. 3 lasted 5 days.
[c] Exp. 6 lasted 9 days.
[d] Additional nutrients were added to all microcosms except to those corresponding to treatment A in Exp. 4.

Exp. 4 and as a result, only the sum of these two fractions is available for this experiment. The percentage of photosynthetically incorporated ^{14}C reallocated during the dark period was determined for each biochemical pool according to:

$$\% \text{ reallocation} = (D_{24} - D_{10}) * 100/D_{10}$$

where D_{24} stands for the ^{14}C incorporation over the 24-h incubation and D_{10} for the ^{14}C incorporation over the 10-h incubation under continous light.

At the start and the end of Exps. 4, 5 and 6, additional incubations were carried out for the study of photosynthesis-irradiance relationships. Seven 70-ml bottles were filled with water from each microcosm, inoculated with 185 kBq (5 μCi) of $NaH^{14}CO_3$ and placed in a refrigerated (18 ± 1 °C) incubator for ca 3 h under natural light. Incubations were performed at noon. A set of neutral density plastic screens provided an irradiance gradient according to 100, 58, 40, 20, 8 and 2% of incident light. One of the incubation bottles, covered with aluminium foil, served as a black bottle. Irradiance was measured during the incubations by means of a 2 sensor connected to a Li-Cor Datalogger. Incubations were stopped by filtering the samples through a GF/F Whatman glass fibre filter (< 100 mm Hg). Inorganic ^{14}C-bicarbonate was removed with 0.1 N HCl as described in Lean & Burnison (1979) and the filters placed in scintillation vials to which 5 ml of scintillation cocktail were added. Counting of the samples was done as previously described. Dark carbon incorporation was not substracted. Photosynthesis-irradiance curves derived from these experiments were fitted to the hyperbolic tangent equation (Platt & Jassby, 1976) when photoinhibition was not observed or to the continuous exponential equation (Platt et al., 1980) when photoinhibition was apparent.

2.3. *Statistical analyses*

In order to test for significant differences in growth rate between treatments during the logarithmic phase of the experiments, Chl *a* concentration values were fitted to a linear regression model ($\log_e$ transformed values were used when exponential growth was apparent), and the slopes of the regression lines compared by means of an analysis of covariance (ANCOVA). One-way analysis of variance (ANOVA) was used in order to test for differences between treatments in the variables monitored along the experiments. Normality of the variables and homogeneity of variances were tested using Kolmogorov-Smirnov and Cochran tests before running the statistical analyses. Multiple comparison between treatments was performed using Student-Newman-Keuls tests. Statistical analyses were undertaken using SAS (Version 6.0, SAS Institute Inc.) and SPSS (Version 4.0, SPSS Inc.) software.

3. Results

3.1. *Field survey*

The vertical distribution of temperature, nitrate concentration, Chl *a* concentration (Chl *a*) and the protein-C:carbohydrate-C (P:C) ratio during the sampling period is

shown in Fig. 1. During the first three cruises (from 12th July to 6th August), the water column was stratified, with surface temperature above 18 °C and nitrate concentration showing values below 1 μmol·l^{-1} in the upper 20 m. Relatively low Chl *a* concentrations (< 0.6 μg·l^{-1}) were measured during this period, and maximum values were found in sub-surface layers. On 14th August, by contrast, surface temperature decreased to 15.6 °C, whereas nitrate concentration increased to more than 4 μM at depths below 10 m. The vertical profile of Chl *a* concentration showed a maximum at the surface (1.3 μg ·l^{-1}), reflecting the effects of upwelling. Thermal stratification of the water column was present again during the next cruise, when a sharp thermocline was located between 10 and 20 m, and nitrate concentration in the upper mixed layer was below 1 μmol· l^{-1}. A conspicuous sub-surface chlorophyll maximum (1.5 μg·l^{-1}) was observed at 30 m depth on 28th August.

Marked differences were found between the distributions of particulate protein and carbohydrate concentrations (data not shown). Prior to the upwelling event, protein-C and carbohydrate-C concentrations ranged from 10 to 30 μg·l^{-1} and 30 to 50 μg·l^{-1}, repectively. As a result, the protein-C:carbohydrate-C (P:C) ratio was < 1 as long as thermal stratification remained, with no clear pattern evident in its vertical profile (Fig. 1). By contrast, a strong vertical gradient was found during the upwelling phase,

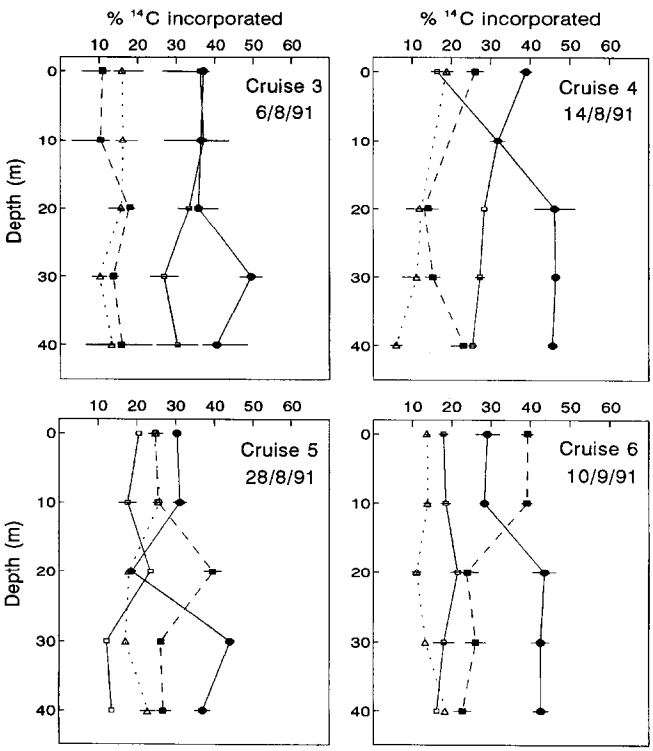

Fig. 2. Vertical profiles of the percentage of ^{14}C incorporated into proteins (●), polysaccharides (□), lipids (■) and low molecular weight metabolites (△) during cruises 3, 4, 5 and 6. Error bars represent ± 1 SE (n = 3).

when the P:C ratio reached values greater than 1 in the upper 20 m of the water column with a marked maximum (2.3) present at surface. Maximum values of the P:C ratio were measured in deeper waters from 14th August onwards, with the highest values being measured at 20 and 30 m on 28th August and 10th September, respectively.

Phytoplankton species composition did not show major changes during this survey. *Chaetoceros* spp., *Rhizosolenia alata* Brightwell and *Leptocylindrus danicus* Cleve were the most abundant diatoms, whereas small *Gymnodinium* and *Gyrodinium* species exhibited the highest densities among dinoflagellates. Microflagellates were numerically the most abundant group in all the cruises.

Primary production was much higher during the upwelling event than in the stratification period. Total carbon incorporation rate integrated over the upper 40 m averaged 247.4 ± 97.8 mgC·m^{-2}·day^{-1} for cruises 3, 5 and 6 (primary production data from cruises 1 and 2 are not available), and 738.7 mgC·m^{-2}·day^{-1} during cruise 4.

Patterns of ^{14}C partitioning into the measured end-products of photosynthesis showed notable differences between cruises (Fig. 2). The largest proportion of ^{14}C was incorporated into the protein fraction in most of the samples. The relative contribution of proteins was maximum during upwelling, when more than 45% of the ^{14}C label appeared

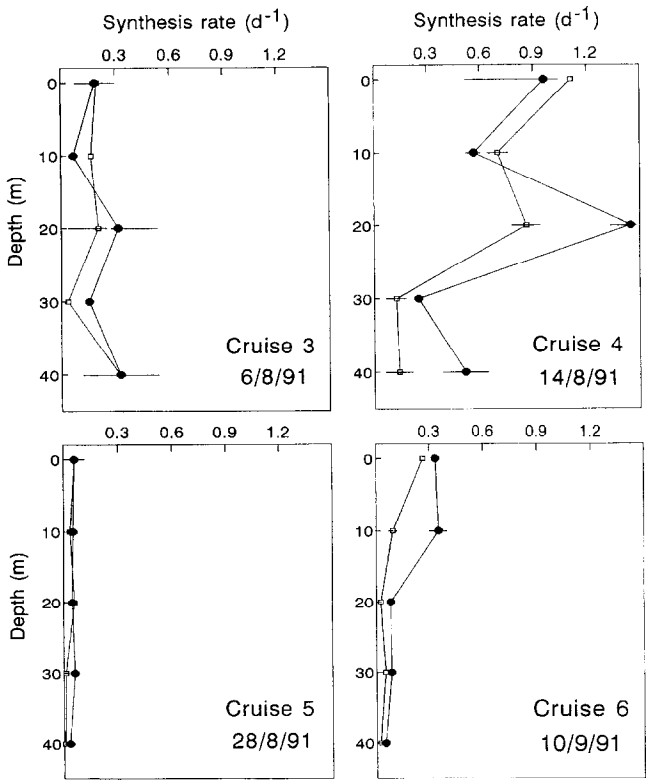

Fig. 3. Vertical profiles of protein (●) and polysaccharide (□) specific synthesis rates during cruises 3, 4, 5 and 6. Error bars represent ± 1 SE ($n = 3$).

in this fraction below 20 m. Relative carbon incorporation into protein showed a consistent increase with depth during the sampling period. The vertical distribution of the percentage of ^{14}C incorporated into the other three fractions displayed less distinct patterns. Carbon incorporation into polysaccharides was relatively high ($\approx 30\%$) during cruises 3 and 4, but decreased in the last two cruises. An opposite trend was observed for lipids, whose relative carbon incorporation increased from less than 20% during cruise 3 to 40% in the surface layer during the last cruise. Values of ^{14}C incorporation into LMWM were usually low, between 10% and 20%, except during cruise 5, when values of about 25% were measured in the upper mixed layer.

Specific synthesis rates of proteins and polysaccharides during cruises 3 to 6 are shown in Fig. 3. The highest rates for both variables occurred during the upwelling event (cruise 4), when values between 0.6 day^{-1} and 1.4 day^{-1} were measured in the upper 20 m of the water column, yielding doubling times for each pool lower than 1 day. During the stratification period, macromolecular synthesis rates remained below 0.4 day^{-1} for all the cruises. The lowest values (<0.07 day^{-1}) were found during upwelling relaxation (cruise 5), coincident with the highest integrated Chl *a* concentration measured during the whole sampling period (Fig. 1).

3.2. *Microcosm experiments*

3.2.1. *Chlorophyll a*, nitrate and species composition

Changes in nitrate and Chl *a* concentration during the six experiments are shown in Table 2 and Fig. 4. Variations in silicate concentration closely paralleled those of nitrate concentration (data not shown), as demonstrated by the significant linear correlation found between these two variables ($r^2 = 0.66$, $p < 0.01$, $n = 199$). Results of the ANCOVAs performed to test for differences in chlorophyll specific growth rates between treatments are shown in Table 3.

Phytoplankton populations enclosed in the microcosms during Exps. 1, 2 and 3 did not display any increase in Chl *a* in spite of the high light and nutrient-rich conditions characteristic of some treatments. In these experiments, Chl *a* concentration decreased in all microcosms (Fig. 4), whereas nitrate concentration maintained its initial high values (Table 2). A different pattern was found in Exps. 4, 5 and 6, in which phytoplankton blooms developed after a 4–5 days lag period.

In microcosms 4A and 4B (Exp. 4, treatments A and B), phytoplankton populations taken from 10 m depth at the sampling station, were incubated under light intensities close to their original irradiance level (300 $\mu E \cdot m^{-2} \cdot s^{-1}$), with (treatment B) and without (treatment A) addition of nutrients (see Table 1). Treatment A simulated the maintenance of the cells in the euphotic layer after an upwelling event, whereas treatment B represented the occurrence of a second upwelling event, thus implying a further nutrient enrichment. In this experiment, very rapid growth started at day 4 and final Chl *a* concentrations of 7.0 ± 0.1 $\mu g \cdot l^{-1}$ in microcosms 4A and 12.5 ± 2.5 $\mu g \cdot l^{-1}$ in microcosms 4B were measured (Fig. 4). The relative abundance of several chain-forming diatoms increased sharply as the experiment progressed. *Chaetoceros* spp., *Thalassiothrix frauenfeldii* Grunow and *Stauroneis membranacea* (Cleve) Hustedt made up the bulk of the phytoplankton biomass, with microflagellates being also numerically

Table 2
Concentration of nitrate in the experimental microcosms

	Microcosm			
	A	B	C	D
Exp. 1				
Day 0	6.1 ± 0.8	5.7 ± 0.3	6.7 ± 0.1	–
Day 4	6.7 ± 0.1	–	5.8 ± 0.4	–
Day 7	5.2 ± 0.3	–	5.7 ± 0.2	–
Exp. 2				
Day 0	7.0 ± 0.9	7.8 ± 0.2	8.6 ± 0.8	7.8 ± 0.3
Day 4	7.0 ± 1.0	7.9 ± 0.1	7.9 ± 0.2	6.5 ± 1.4
Day 7	8.4 ± 0.2	8.0 ± 0.2	8.1 ± 0.2	7.9 ± 0.2
Exp. 3				
Day 0	6.2 ± 0.7	6.4 = 0.1	5.5 ± 0.6	5.7 ± 0.4
Day 3	3.8 = 2.0	6.0 ± 0.5	6.1 ± 0.0	5.8 = 0.0
Day 5	5.8 = 0.1	5.3 ± 0.6	5.9 ± 0.4	5.6 = 0.4
Exp. 4				
Day 0	6.1 ± 0.4	8.9 ± 1.0	12.1 ± 0.2	11.5 ± 0.4
Day 4	4.8 = 0.3	8.9 ± 0.9	10.9 ± 0.6	11.6 ± 0.2
Day 7	1.2 ± 0.4	0.3 = 0.2	9.9 ± 1.3	12.0 ± 0.1
Exp. 5				
Day 0	5.4 ± 0.1	5.7 ± 0.5	5.4 = 0.2	6.3 ± 0.7
Day 4	5.2 ± 0.3	5.8 ± 0.6	5.0 ± 0.4	4.6 ± 0.4
Day 7	5.3 ± 0.1	2.6 ± 0.3	2.1 ± 1.2	3.8 ± 1.9
Exp. 6				
Day 0	7.6 ± 1.8	6.1 ± 0.1	6.9 ± 0.7	6.0 ± 0.1
Day 5	8.8 ± 2.3	6.0 ± 0.1	7.4 ± 1.6	5.7 ± 0.1
Day 9	7.7 ± 1.7	1.2 ± 0.9	0.3 ± 0.2	0.1 ± 0.0

Concentration is expressed as $\mu mol \cdot l^{-1}$ (mean ± 1 SE, $n = 3$).

important. In these microcosms, nitrate levels fell sharply during the incubation period, but they did not show any major change in 4C and 4D microcosms (Table 2). In this experiment (Exp. 4), treatments C and D simulated two velocities of decreasing irradiance (Table 1). A slight increase in Chl *a* concentration occurred in C microcosms, whereas no change was recorded in D microcosms. However, there were no significant differences in either growth rate (ANCOVA, $p > 0.3$, Table 3) or final Chl *a* values (ANOVA, $p > 0.05$) between these two microcosms. Growth rate during the second half of this experiment (days 4–7), as estimated from the slope of the regression line of $\log_e$ Chl *a* concentration versus time, was significantly higher in 4A and 4B microcosms than in 4C and 4D microcosms (ANCOVA, $p < 0.05$, see Table 3).

In Exps. 1, 2, 3, 5 and 6, microcosms B, C and D ("upwelling" microcosms) were exposed to different velocities of increasing irradiance simulating an upwelling event, whereas treatment A ("control") corresponded to the maintenance of phytoplankton populations [taken from 30 m depth (Exp. 5) and 20 m depth (Exp. 6)] under their

Table 3
Results from the regression and covariance analyses performed on the Chl *a* concentration values from the experimental microcosms

	Microcosm	Time period (days)	df	*b*	*r*	*p*	df′	*p*′	Differences in slope between treatments (absolute values)
Exp. 1									
	1A	0–7	22	−0.035	0.82	**	1	**	$b3 > b1$
	1B	0–7	23	−0.054	0.94	**			
Exp. 2									
	2A	0–7	22	−0.11	0.91	**	3	**	$b1 = b2 = b3$
	2B	0–7	22	−0.11	0.95	**			$b2 = b3 > b4$
	2C	0–7	22	−0.14	0.95	**			
	2D	0–7	22	−0.07	0.65	**			
Exp. 3									
	3A	0–5	16	−0.20	0.76	**	3	n.s.	$b1 = b2 = b3 = b4$
	3B	0–5	16	−0.33	0.90	**			
	3C	0–5	16	−0.19	0.79	**			
	3D	0–5	16	−0.18	0.56	*			
Exp. 4									
	4A	4–7	10	0.50	0.97	**	3	*	$b1 = b2 > b3 = b4$
	4B	4–7	10	0.61	0.87	**			
	4C	4–7	10	0.27	0.70	*			
	4D	4–7	10	0.10	0.18	n.s.			
Exp. 5									
	5A	3–7	13	0.02	0.06	n.s.	3	*	$b1 < b2 = b3 = b4$
	5B	3–7	13	0.36	0.59	*			
	5C	3–7	13	0.38	0.76	**			
	5D	3–7	13	0.38	0.73	**			
Exp. 6									
	6A	5–9	13	0.24	0.55	*	3	***	$b1 < b2 = b3 = b4$
	6B	5–9	13	0.88	0.94	**			
	6C	5–9	13	0.46	0.87	**			
	6D	5–9	13	0.65	0.92	**			

For Exps. 1 and 2, Chl *a* concentration values were fitted to linear models. Logarithm transformed ($\log_e$) values were used in the case of Exps. 3 to 6. Only those data belonging to the growth phase were included in the analysis for Exps. 4 to 6. df = Degrees of freedom in the regression analysis; b = slope of the regression line; r = regression coefficient; p = significance value of the regression coefficient; df′ = degrees of freedom in the analysis of covariance performed to test for differences in the slope of the regression line; p' = significance of the comparison between slopes. *, $p < 0.05$; **, $p < 0.01$; ***, $p < 0.001$. n.s. = not significant.

original irradiance level ($\approx 30\ \mu E \cdot m^{-2} \cdot s^{-1}$) (see Table 1). The concentration of Chl *a* decreased steadily throughout Exps. 1, 2 and 3, for all the treatments tested (Fig. 4). Changes in chlorophyll concentration were similar in Exps. 5 and 6, even though exponential growth rates and final Chl *a* values were higher in Exp. 6 (Fig. 4). In both experiments, chlorophyll levels did not show any major changes in "control" micro-

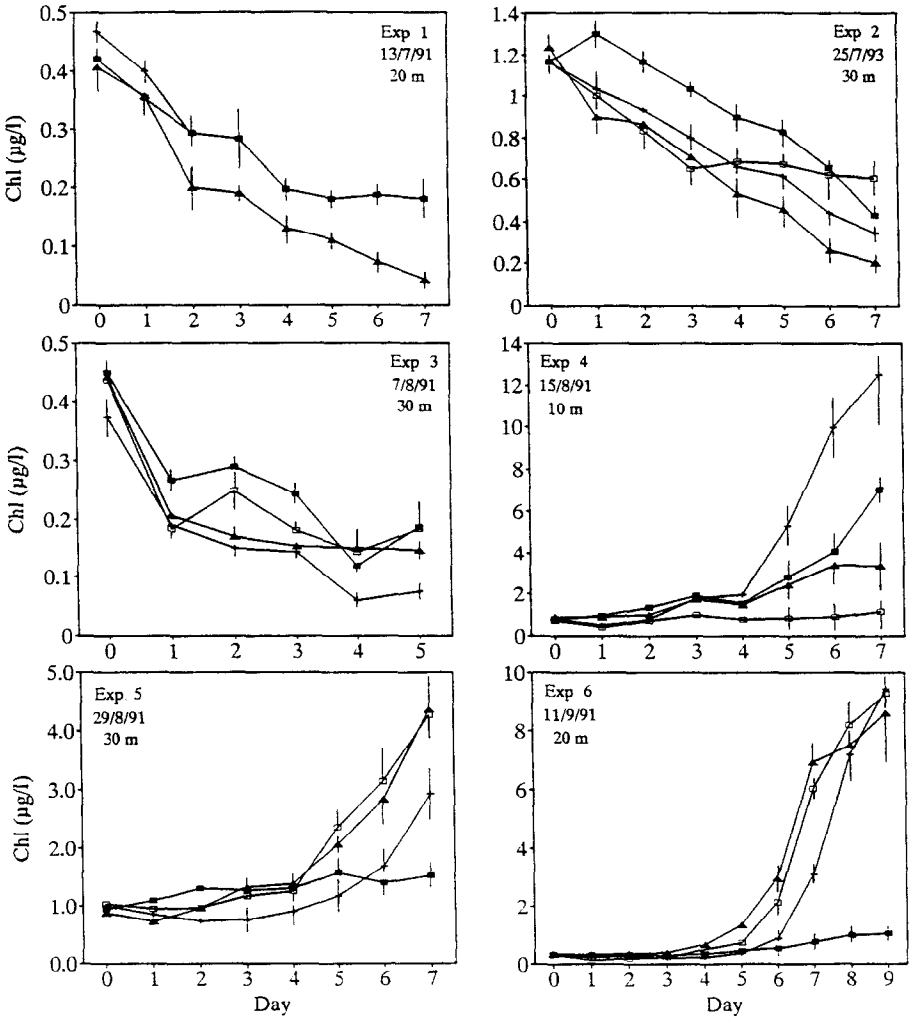

Fig. 4. Changes in chlorophyll *a* concentration in the experimental microcosms. Error bars represent ± 1 SE ($n = 3$). Note differences in *y*-axis scale. Date and depth from where samples were taken are also indicated. In Exp. 4, phytoplankton assemblages were incubated at their original irradiance level without (A microcosms) and with (B microcosms) addition of nutrients, or exposed to decreasing levels of irradiance simulating a downward movement of the water body at a velocity of 6 m·day^{-1} (C microcosms) and 9 m·day^{-1} (D microcosms). In Exps. 1, 2, 3, 5 and 6, microalgae were incubated at their original irradiance level (A microcosms) or exposed to increases in irradiance simulating upwelling of the water at a velocity of 6 m·day^{-1} (B microcosms), 8 m·day^{-1} (C microcosms) and 30 m·day^{-1} (D microcosms). See methods and Table 1 for details. (■), A microcosms; (+), B microcosms; (▲), C microcosms; (□), D microcosms.

cosms, whereas substantial increases in "upwelling" microcosms occurred during the last 3–4 incubation days. Changes in nitrate concentration followed an opposite trend to those of chlorophyll concentration. Nitrate levels did not vary largely in 5A and 6A ("control") microcosms, but they decreased noticeably in the other microcosms

(Table 2). This decrease was higher in 6C and 6D microcosms, where values below 0.5 $\mu mol \cdot l^{-1}$ were measured at the end of the incubation.

In Exp. 5, final Chl *a* values above 4.2 $\mu g \cdot l^{-1}$ were measured in 5C and 5D microcosms, whereas at the end of Exp. 6, Chl *a* levels were higher than 8.5 $\mu g \cdot l^{-1}$ in 6B, 6C and 6D microcosms. Microcosms 5B, 5C and 5D, where upwelling was simulated, showed significantly higher final chlorophyll concentration (ANOVA, $p < 0.05$) and growth rate (ANCOVA, $p < 0.05$, Table 3) than 5A microcosms, where initial irradiance conditions were maintained. Similarly, Chl *a* concentration at the end of the incubation in 6B, 6C and 6D microcosms was also significantly higher than in 6A microcosms (ANOVA, $p < 0.01$). In both Exps. 5 and 6, the relative abundance of diatoms increased towards the last days of the incubation. The most abundant phytoplankton species present in Exp. 5 were the diatoms *Nitzschia closterium* (Ehrenberg) W. Smith and *Thalassiosira* spp., along with the dinoflagellate *Gymnodinium* spp. The high chlorophyll values measured in Exp. 6 were mainly due to a small *Chaetoceros* spp. and *Nitzschia closterium*. High numbers of microflagellates were also found in all these microcosms.

3.2.2. *Protein-C: carbohydrate-C ratio*

Values of the protein-C:carbohydrate-C (P:C) ratio during Exps. 3 to 6 are shown in Table 4. This ratio increased slightly during Exp. 3 reaching values higher than 1 in 3A and 3B microcosms. No significant differences were found among treatments

Table 4
Protein-C:carbohydrate-C ratio in the experimental microcosms 3 to 6 (mean ± 1 SE, $n = 3$)

	Microcosms			
	A	B	C	D
Exp. 3				
Day 0	0.42	0.42	0.42	0.42
Day 3	0.52 ± 0.01	0.56 ± 0.08	0.92 ± 0.47	0.63 ± 0.03
Day 5	1.03 ± 0.13	1.2 ± 0.16	0.79 ± 0.14	0.57 ± 0.1
Exp. 4				
Day 0	1.32 ± 0.21	1.32 ± 0.21	1.32 ± 0.21	1.32 ± 0.21
Day 4	2.38 ± 0.09	1.75 ± 0.15	1.11 ± 0.11	1.34 ± 0.30
Day 7	0.51	5.54 ± 0.87	1.19 ± 0.21	1.16
Exp. 5				
Day 0	0.62 ± 0.13	0.62 ± 0.13	0.62 ± 0.13	0.62 ± 0.13
Day 4	0.57 ± 0.05	0.74 ± 0.33	3.21 ± 1.16	1.24 ± 0.41
Day 7	0.84 ± 0.09	6.02 ± 0.68	2.29 ± 0.52	1.34 ± 0.23
Exp. 6				
Day 0	0.54 ± 0.07	0.54 ± 0.07	0.54 ± 0.07	0.54 ± 0.07
Day 5	1.56 ± 0.23	0.44 ± 0.02	3.02 ± 0.42	2.48 ± 0.08
Day 9	0.96 ± 0.14	0.67	0.75 ± 0.07	0.59

Biochemical composition data from the microcosms were not available at the start of the experiments. Day 0 values in the table refer to the ratios calculated for the water used as inoculum for the experiments.

(ANOVA, $p > 0.07$) in this experiment. The highest initial values were recorded in Exp. 4 (1.3 ± 0.2). In 4A ("control") microcosms, this ratio peaked on day 4 (2.4 ± 0.1) then decreasing towards the end of the incubation, whereas in 4B microcosms it increased steadily until the end of the experiment, when a very high value was measured (5.5 ± 0.9). In Exp. 5, the P:C ratio increased in "upwelling" microcosms. This increase was larger in 5B (6.0 ± 0.7 on day 7) and 5C (2.3 ± 0.5 on day 7) microcosms. In contrast, no major changes of the ratio were observed in microcosm 5A. In Exp. 6, a noticeable increase in the P:C ratio was found in 6C and 6D microcosms, where it was significantly higher on day 5 (SNK tests, $p < 0.05$). By the end of the experiment, this ratio decreased to values below 1 in 6A, 6C and 6D microcosms, and increased slightly in 6B microcosms, but differences between treatments were not significant (ANOVA, $p > 0.16$).

3.2.3. *Photosynthesis-irradiance relationships*

Photosynthetic parameters estimated from the photosynthesis-irradiance experiments conducted at the start and end of Exps. 4, 5 and 6 are shown in Table 5. In general, P^Bmax increased at the end of the incubations in all the microcosms. This increase was larger in those enclosures where actively growing phytoplankton populations dominated (e.g. 4B, 5D and 6D microcosms). In Exp. 4, P^Bmax showed a 4-fold increase in

Table 5
Photosynthetic parameters of the photosynthesis-irradiance (P-I) curves for Exps. 4, 5 and 6

	P^Bmax		α^B	
	Day 0	Day 7	Day 0	Day 7
Exp. 4				
4A	1.61 (±0.26)	1.69 (±0.30)	0.0178 (±0.0073)	0.0357 (±0.0158)
4B	1.00 (±0.12)	4.56 (±0.48)	0.0169 (±0.0057)	0.0303 (±0.0111)
4C	1.21 (±0.13)	1.96 (±0.23)	0.0181 (±0.0063)	0.0324 (±0.0192)
4D	1.19 (±0.17)	1.57 (±0.18)	0.0206 (±0.0103)	0.0217 (±0.0106)
Exp. 5				
5A	2.85 (±0.19)	2.61 (±0.22)	0.0422 (±0.0079)	0.0212 (±0.0064)
5B	2.33 (±0.45)	3.37 (±0.39)	0.0210 (±0.0155)	0.0250 (±0.0099)
5C	3.12 (±0.27)	3.39 (±0.17)	0.0425 (±0.0119)	0.0256 (±0.0045)
5D	2.82 (±0.25)	4.14 (±0.44)	0.0302 (±0.0111)	0.0252 (±0.0080)
	Day 0	Day 9	Day 0	Day 9
Exp. 6				
6A	1.33 (±0.19)	4.19 (±0.46)	0.0368 (±0.0263)	0.0075 (±0.0027)
6B	1.02 (±0.15)	6.32 (±0.99)	0.0270 (±0.0197)	0.0135 (±0.0075)
6C	1.42 (±0.17)	6.11 (±0.80)	0.0279 (±0.0180)	0.0131 (±0.0060)
6D	1.15 (±0.17)	8.02 (±1.15)	0.0409 (±0.0321)	0.0125 (±0.0056)

P^Bmax = maximum chlorophyll-normalized photosynthetic rate [$\mu gC \cdot \mu gChl^{-1} \cdot h^{-1}$]; α^B = initial slope of the P-I curve [$\mu gC \cdot \mu gChl^{-1} \cdot h^{-1} \cdot (\mu E \cdot m^{-2} \cdot s^{-1})^{-1}$]. Upper and lower 95% asymptotic confidence limits are shown in parentheses.

4B microcosms, where a diatom bloom occurred, displaying a value of 4.5 μgC·μgChl^{-1}·h^{-1} at the end of the incubation. A significant increase was also measured during Exp. 5 in "upwelling" microcosms, parallelling increases in phytoplankton biomass. The largest increase took place in 5D microcosms, where phytoplankton cells experienced the sharpest irradiance changes. On the other hand, this parameter decreased slightly in "control" microcosms, where phytoplankton populations were incubated at their original, low irradiance conditions and no growth was observed. P^Bmax values at the start of Exp. 6 were similar to those measured at the beginning of Exp. 4. At the end of Exp. 6, much higher values of P^Bmax were measured in all the microcosms. This increase in P^Bmax was particularly significant in 6D microcosms, where a 7-fold increase took place by the end of the experiment.

The initial slope of the P-I curve, α^B, displayed an increase in all microcosms at the end of Exp. 4, whereas the opposite was observed in Exps. 5 and 6, with the exception of 5B microcosms. Differences in α^B values among treatments were not significant in any case, due to the large range of the confidence intervals. Lack of accuracy in the estimation of α^B was mainly due to the use of a small number of low irradiance ($< 10\%$ I_0) levels assayed during the P-I experiments.

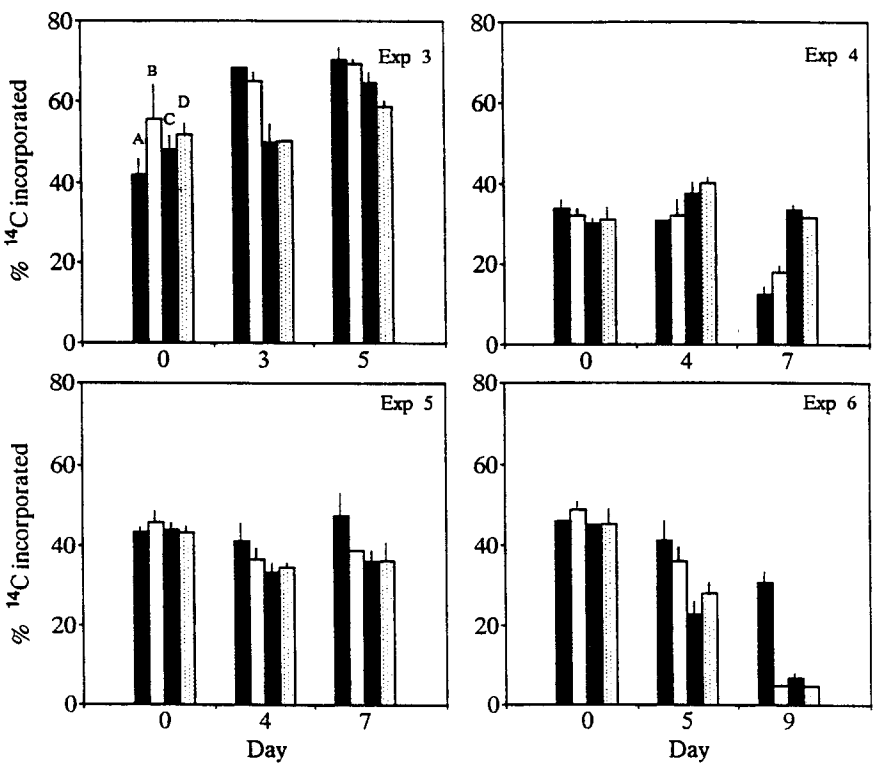

Fig. 5. Percentage of ^{14}C incorporated into proteins in the experimental microcosms during Exps. 3, 4, 5 and 6. Error bars represent $\pm$ 1 SE ($n = 3$).

3.2.4. ^{14}C-labelling patterns

The percentage of ^{14}C incorporated into the protein fraction during Exps. 3 to 6 is shown in Fig. 5. In general, changes in relative carbon incorporation into protein followed an opposite trend to those of Chl *a* concentration (Fig. 4). During Exp. 3, this percentage increased in all the microcosms, reaching values above 60% at the end of the incubation. Lower values were measured during Exp. 4, where a sharp decrease took place in 4A and 4B microcosms, coinciding with an increase in phytoplankton growth and concomitant nitrate depletion (see Fig. 4 & Table 2). In 4C and 4D microcosms, the relative incorporation of ^{14}C into protein maintained its initial value ($\approx 38\%$) throughout the experimental period, and similarly, chlorophyll and nitrate concentration showed only very slight variations. At the end of the experiment, the relative carbon incorporation into protein in these microcosms was significantly higher than in 4A and 4B microcosms (ANOVA, $p < 0.001$; SNK test).

Changes in the percentage of ^{14}C incorporated into protein during Exp. 5 were small. This percentage increased slightly in "control" microcosms, and decreased to values below 40% in "upwelling" microcosms by the end of the incubation, although differences between treatments were not significant (ANOVA, $p > 0.3$). A similar pattern was found in Exp. 6, as the relative carbon incorporation into protein did not change in 6A microcosm, where phytoplankton growth was not observed. By contrast, an 8-fold decrease in the percentage of ^{14}C incorporated into proteins was measured at the end of the experiment in 6B, 6C and 6D ("upwelling") microcosms, where growing phytoplankton assemblages developed and nitrate depletion occurred. At the end of the incubation period, the percentage of ^{14}C flowing into protein in these enclosures was significantly lower than in 6A microcosm (ANOVA, $p < 0.05$, SNK test).

Changes in the percentage of ^{14}C incorporated into polysaccharides during the experiments were not as marked as those changes in the relative incorporation of carbon into protein (Fig. 6). In most cases, differences between treatments were not significant. In Exp. 3, relative ^{14}C incorporation into polysaccharides decreased in 3A and 3B microcosms, with all treatments showing similar final values ($\approx 15\%$). This percentage also diminished throughout Exp. 4, where initial values above 30% were reduced to near 20% at the end of the incubation. The lowest relative carbon incorporation into polysaccharides occurred during Exp. 5, where this proportion took values of about 10% in all microcosms. In Exp. 6, initial values were higher ($\approx 20\%$), and no remarkable temporal changes were detected.

The percentages of ^{14}C incorporation into lipids and low molecular weight metabolites (LMWM) during Exps. 3–6 are shown in Table 6. Relative carbon incorporation into lipids showed rather low values ($< 14\%$) at the start of Exp. 3, and decreased thereafter in all treatments. This percentage showed a small decrease in 3A, 3B and 3C microcosms, whereas it increased slightly in 3D microcosms. The sum of the relative carbon incorporation into lipid and LMWM fractions exhibited values close to 35% at the start of Exp. 4. This percentage increased sharply in 4A and 4B microcosms, reaching values up to 60% at the end of the experiment, whereas a smaller increase occurred in 4C and 4D microcosms. By day 7, the relative amount of ^{14}C incorporated into these fractions in 4A and 4B microcosms was significantly higher than in 4C and 4D microcosms (ANOVA, $p < 0.001$, SNK test).

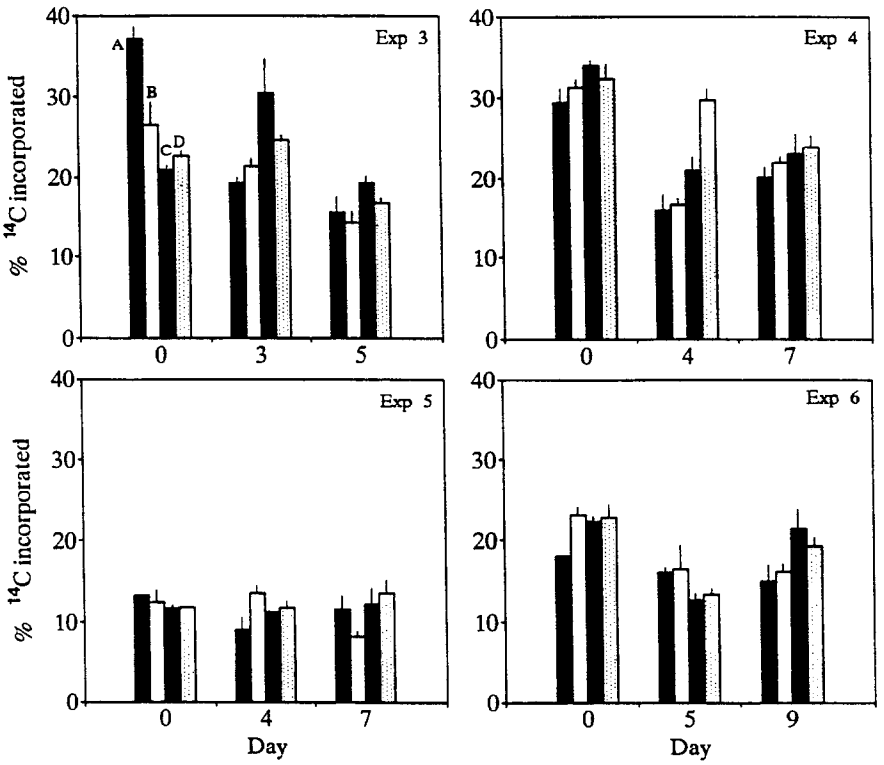

Fig. 6. Percentage of ^{14}C incorporation into polysaccharides in the experimental microcosms during Exps. 3, 4, 5 and 6. Error bars represent ± 1 SE ($n = 3$).

The relative incorporation of ^{14}C into lipids in 5B, 5C and 5D ("upwelling") microcosms increased from $\approx 15\%$ on day 0 to $\approx 25\%$ on day 7, but did not show notable changes in 5A ("control") microcosms. By the end of the experiment, relative ^{14}C incorporation into lipids in 5A microcosms was significantly lower than in the other microcosms (ANOVA, $p < 0.05$, SNK test). The relative synthesis of LMWM took values close to 30% throughout this experiment, and differences between treatments at the end of the incubation were not significant (ANOVA, $p > 0.8$). During Exp. 6, relative ^{14}C incorporation into lipids showed a slight increase in all microcosms. At the end of the experiment, relative synthesis of lipids in "upwelling" microcosms was close to 15%, significantly lower than in "control" microcosms, where a percentage $> 20\%$ was measured (SNK test, $p < 0.05$). The percentage of ^{14}C incorporated into LMWM in 6A microcosm was about 30% throughout the experiment. This percentage increased sharply in 6B, 6C and 6D ("upwelling") microcosms, reaching values close to 60%, coinciding with very low nitrate levels (Table 2) and relative ^{14}C incorporation into proteins (Fig. 4).

Table 6
Percentage of ^{14}C incorporation into lipids (LIP) and low molecular weight metabolites (LMWM) in the experimental microcosms (mean ± 1 SE, $n = 3$)

	% LIP				% LMWM			
	3A	3B	3C	3D	3A	3B	3C	3D
Exp. 3								
Day 0	8.0 ± 2.5	5.4 ± 1.7	13.5 ± 0.7	13.2 ± 1.2	12.8 ± 3.9	12.3 ± 1.2	17.2 ± 2.0	12.2 ± 3.3
Day 3	4.1 ± 0.8	5.1 ± 1.1	7.3 ± 1.9	9.2 ± 4.6	8.0 ± 0.3	8.6 ± 0.1	12.3 ± 1.8	19.8 ± 2.5
Day 5	2.8 ± 1.0	5.2 ± 0.3	5.6 ± 1.7	10.5 ± 0.2	8.5 ± 1.2	10.9 ± 0.1	10.5 ± 1.1	14.2 ± 1.5
			% (LIP + LMWM)					
			4A	4B	4C	4D		
Exp.4								
Day 0			34.6 ± 1.0	36.6 ± 0.4	34.7 ± 1.2	34.4 ± 4.3		
Day 4			53.1 ± 2.9	51.2 ± 2.0	41.4 ± 4.0	30.1 ± 2.7		
Day 7			67.4 ± 2.7	60.2 ± 1.8	43.5 ± 2.5	44.5 ± 1.7		
	% LIP				% LMWM			
	5A	5B	5C	5D	5A	5B	5C	5D
Exp. 5								
Day 0	16.7 ± 1.2	16.0 ± 1.1	17.3 ± 0.6	18.1 ± 0.5	24.4 ± 0.1	25.9 ± 0.2	27.3 ± 1.2	27.0 ± 1.9
Day 4	20.6 ± 1.0	22.7 ± 1.1	22.5 ± 0.8	22.4 ± 0.8	29.4 ± 2.4	27.3 ± 2.3	33.1 ± 2.8	31.3 ± 1.1
Day 7	17.5 ± 3.7	27.6 ± 1.5	24.8 ± 0.9	26.4 ± 1.3	23.7 ± 4.3	25.5 ± 1.1	27.1 ± 2.9	24.1 ± 2.8
	% LIP				% LMWM			
	6A	6B	6C	6D	6A	6B	6C	6D
Exp. 6								
Day 0	14.2 ± 0.7	8.6 ± 0.4	10.9 ± 0.2	10.7 ± 1.1	23.1	19.5 + 1.2	21.8 + 1.1	21.1 ± 1.4
Day 5	15.1 ± 0.5	16.9 ± 0.1	16.4 ± 1.6	14.8 ± 1.3	27.6 ± 2.7	30.7 ± 5.6	48.3 ± 2.0	42.3 ± 4.1
Day 9	20.5 ± 1.7	14.8 ± 1.5	13.6 ± 0.4	15.1 ± 1.4	33.8 ± 3.5	64.3 ± 3.1	58.2 ± 6.4	61.0 ± 2.6

Due to methodological problems, only the sum of the two fractions is available for Exp. 4 (see Methods).

3.2.5. Dark ^{14}C-reallocation patterns

The percentages of dark ^{14}C reallocation in the protein and polysaccharide fractions during Exps. 4 and 5 are shown in Table 7. At the start of Exp. 4, rates of protein synthesis in darkness were similar to those measured during the light period, as indicated by percentages of dark ^{14}C reallocation around 100. As the experiment progressed, protein labelling during the dark decreased sharply in all microcosms. The most pronounced decrease occurred in 4D microcosms, where irradiance levels declined sharply. In these microcosms, proteins were even catabolized during the dark on day 7. By contrast, initial negative values were measured in Exp. 5, where the phytoplankton

Table 7
Dark ^{14}C reallocation patterns (%) for proteins and polysaccharides in the experimental microcosms 4 and 5 (mean ± 1 SE, $n = 3$)

	Protein				Polysaccharide			
	A	B	C	D	A	B	C	D
Exp. 4								
Day 0	99 ± 23	93	106 ± 21	86	–	–	– 16	– 33.2 ± 3.5
Day 4	100 ± 8	65 ± 10	56	41 ± 3	– 60 ± 2	– 52 ± 6	– 27 ± 3	– 16.7 ± 7.2
Day 7	27 ± 0	31 ± 2	20 ± 9	– 16 ± 5	– 16 ± 2	– 59 ± 12	– 51 ± 18	– 36.3 ± 15.4
Exp. 5								
Day 0	– 27 ± 1	– 31 ± 6	– 32 ± 20	– 35 ± 2	– 54 ± 0	– 47 ± 23	– 53 ± 7	– 53.5 ± 10.0
Day 4	8 ± 2	– 14 ± 8	20 ± 1	5 ± 3	– 59 ± 7	– 55 ± 4	– 62 ± 2	– 62.1 ± 4.3
Day 7	41 ± 18	117 ± 24	62 ± 14	41 ± 13	– 35 ± 6	– 53 ± 8	– 31 ± 4	– 45.1 ± 2.5

For details on calculations, see Methods.

populations from the sub-surface chlorophyll maximum (SCM) were exposed to three different rates of increasing irradiance. This reveals that up to 30% of the radioactive label incorporated into proteins during the light period was reallocated or respired during the dark in the phytoplankton assemblages inhabiting the SCM. This situation changed sharply in all microcosms as the incubation progressed, so that relatively high values of dark protein synthesis were measured at the end of this experiment. Rates of ^{14}C incorporation into protein in darkness even exceeded those measured during the light period in 5B microcosms.

A highly significant decrease in ^{14}C incorporation into polysaccharides during the night was found in all microcosms during Exps. 4 and 5. Percentages of night reallocation, albeit always negative, did not show any distinct variation pattern during Exp. 4. In Exp. 5, initial reallocation values were close to −50%, and only moderate changes occurred throughout the incubation.

3.2.6. Protein and polysaccharide specific synthesis rates

Changes in the specific synthesis rate (SSR) of proteins and polysaccharides are shown in Figs. 7 and 8, respectively. During Exp. 3, specific carbon incorporation rates into proteins and polysaccharides in all microcosms reached values lower than 0.2 day^{-1} and 0.1 day^{-1} respectively throughout the incubation. Differences between microcosms were not significant in any case (ANOVA, $p > 0.05$).

The highest SSR values found throughout this study were measured in Exp. 4, when phytoplankton populations sampled from upwelled waters were incubated at either their original irradiance (4A and 4B microcosms) or decreasing irradiance values (4C and 4D microcosms). Protein SSR increased on day 4 in 4B microcosms, whereas it decreased markedly in 4D microcosms. At the end of the incubation, protein SSR was significantly lower in 4D microcosms than in the other experimental bottles (ANOVA, $p < 0.01$, SNK test). Polysaccharide SSR maintained its high, initial values thoroughout the incubation in 4A and 4B microcosms, paralleling growth of phytoplankton. In

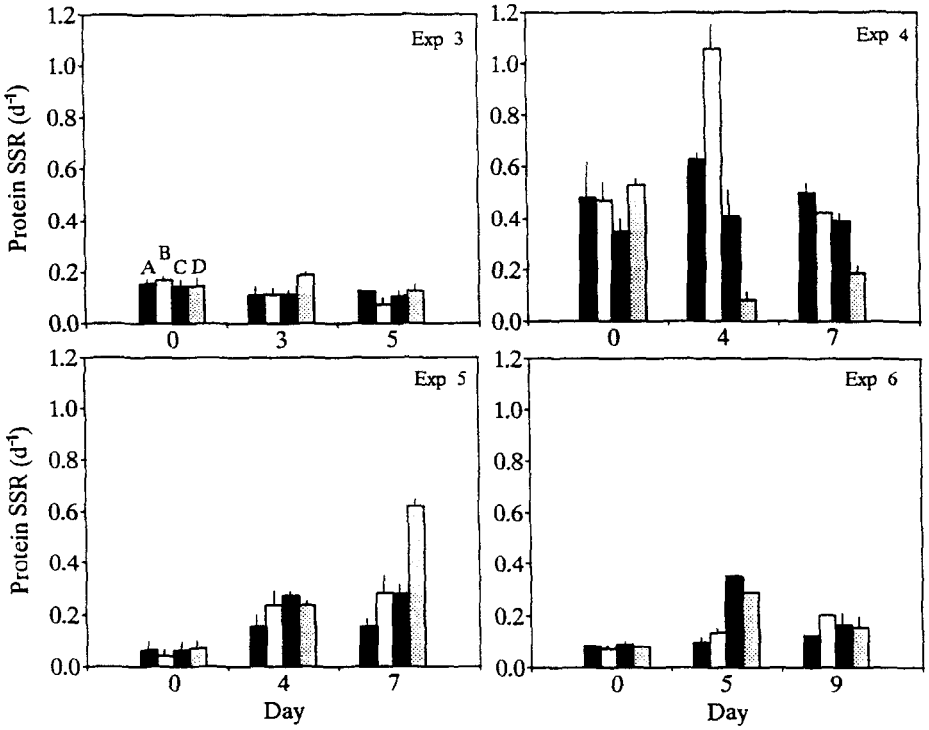

Fig. 7. Protein specific synthesis rate (SSR) in the experimental microcosms during Exps. 3, 4, 5 and 6. Error bars represent ± 1 SE ($n = 3$).

contrast, it decreased drastically in 4C and 4D microcosms, where final values were lower than 0.1 day^{-1}.

During Exp. 5, protein SSR increased in all microcosms. This increase was more important in 5D microcosms, where significantly higher values were measured at the end of the incubation (ANOVA, $p < 0.01$, SNK test). Polysaccharide SSR was very low at the start of this experiment, and increased progressively in 5C and 5D microcosms. At the end of the experiment, specific carbon incorporation into polysaccharide was significantly higher in 5C microcosms (ANOVA, $p < 0.01$, SNK test). Both protein and polysaccharide SSRs exhibited a sharp increase in 6C and 6D microcosms by day 5, when they reached values significantly higher than those of 6A and 6B microcosms (ANOVA, $p < 0.05$, SNK test). By the end of the Exp. 6, specific carbon incorporation into proteins and polysaccharides were similar in all microcosms.

4. Discussion

The combined use of in situ observations and experimental manipulations in microcosms allowed us to examine the physiological changes of microalgae during the advection-relaxation phases characteristic of upwelling systems.

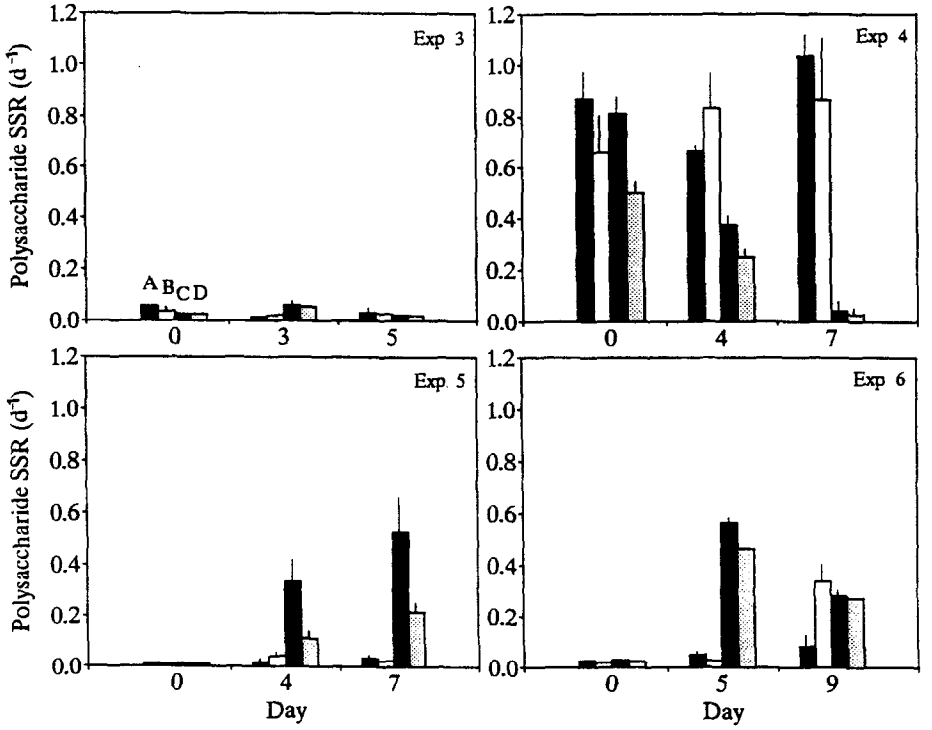

Fig. 8. Polysaccharide specific synthesis rate (SSR) in the experimental microcosms during Exps. 3, 4, 5 and 6. Error bars represent ± 1 SE ($n = 3$).

The existence of a sub-surface chlorophyll maximum (SCM) was a feature of the vertical distribution of chlorophyll concentration when upwelling was absent (Fig. 1). Phytoplankton assemblages which inhabited the SCM showed extremely low turnover rates for proteins and polysaccharides (< 0.1 day^{-1}), yielding duplication times higher than 15 days (Fig. 3). These low turnover rates are not likely to be caused by the presence of high densities of heterotrophs and/or a high concentration of detrital material, since the mean Chl *a* to protein-N ratio measured at the SCM was 2.49 ± 0.11, a value close to that reported by Dortch & Packard (1989) for samples of very high phytoplankton content. High doubling times, together with the relatively low total carbon incorporation rate (4.1 μgC·l^{-1}·day^{-1}) and P:C ratio (0.61) determined for these populations, lead us to conclude that phytoplankton assemblages at the SCM were in a non-growing state, and therefore that accumulation of algae due to increased cell buoyancy and/or reduction of sinking rates at the pycnocline could be the possible mechanisms leading to the formation of this maximum. However, and despite the lack of growth observed in the SCM, the results of Exps. 5 and 6, where increasing irradiance levels simulated upward motion of water, demonstrated that sub-surface phytoplankton populations have the potential for growth in response to upwelling events, originating the development of diatom blooms (see Fig. 4).

During the phase of vertical stratification of the water column in summer 1991, the low protein SSR values (<0.3 day^{-1}) and P:C ratios (<1) (Figs. 1 and 3) were indicative of slow phytoplankton growth. Similar metabolic patterns were found in those experimental microcosms where no phytoplankton growth was detected. During Exps. 1, 2 and 3, sub-surface phytoplankton populations did not show any growth in response to increasing irradiance and nutrient levels (Fig. 4), in spite of the presence of bloom-forming diatoms such as *Chaetoceros* spp. and *Leptocylindrus danicus* in these microcosms. These observations suggest that, in addition to physical stability, irradiance and nutrient availability, other factors may also be relevant in controlling phytoplankton responses to upwelling, at least in enclosed experimental ecosystems. Similar findings have been reported for spring diatom blooms (Fernández et al., 1992). In this connection, temperature has proved to be a significant factor governing the time-lag prior to phytoplankton growth after a simulated upwelling pulse (Ishizaka et al., 1983). Similarly, the incorporation of photosynthetically fixed carbon into cellular compounds may be influenced by the spectral characteristics of light (Rivkin, 1989). Although these factors were not considered in the present study, they are not likely to exert a large effect on the lack of growth observed in the first three experiments, as both temperature and light quality remained constant during the whole sampling period.

In those microcosms where phytoplankton growth was not observed and nitrate concentration was high (i.e. Exp. 3 microcosms), a large proportion of the carbon incorporated photosynthetically was channeled into the protein fraction (Fig. 5), reaching values as high as 60% at the end of Exp. 3. Furthermore, non-growing phytoplankton assemblages in 6A ("control") microcosms maintained their initial, high values of relative ^{14}C incorporation into protein, a similar pattern to that found in "control" microcosms of Exps. 4 and 5. These results strongly support the view that phytoplankton cells tend to maintain protein synthesis rather than storage products synthesis under adverse environmental conditions (Morris et al., 1974; Morris, 1981; Barlow, 1984). Moreover, the vertical distribution of the relative carbon incorporation into protein displayed a consistent pattern throughout the study: highest values were measured below 20 m depth (Fig. 2). This is in agreement with the observation that protein synthesis increases relative to the synthesis of other compounds when irradiance is low (Morris & Skea, 1978; Li & Harrison, 1982; Hawes, 1990).

P^Bmax increased noticeably in all the microcosms where upwelling was simulated, reflecting adaptation of phytoplankton cells to increased light conditions. A marked increase in protein and polysaccharide SSR also took place during the development of phytoplankton blooms (Figs. 7 & 8). Increased protein SSR has previously been found in diatom blooms enclosed in microcosms (Hitchcock, 1978; Hama et al., 1988; Fernández et al., 1992) and is directly related to an increase in growth rate (Lancelot et al., 1986; Di Tullio & Laws, 1983). Parallelling increases in protein SSR during Exp. 5, the synthesis of protein in darkness became noticeable, as revealed by the high, positive values of the percentage of dark ^{14}C reallocation (Table 7). Polysaccharides were metabolized during the dark in all microcosms (Table 7). This result supports previous reports that protein synthesis during dark periods may be sustained by polysaccharide catabolism during phytoplankton growth (Morris & Skea, 1978; Cuhel et al., 1984; Smith et al., 1990). It is interesting to note that proteins were also metabo-

lized during the night at the start of Exp. 5, indicating that phytoplankton populations at the SCM were catabolizing proteins in addition to polysaccharides.

Variations in the biochemical composition of particulate matter were also apparent in microcosms where phytoplankton cells were growing at high rates. The P:C ratio reached values well above 1 (Table 4). In Exp. 6, this ratio decreased sharply at the end of the incubation, when very low nitrate concentrations were measured. This observation is in agreement with the low protein to carbohydrate ratios measured in diatom cultures (Myklestad & Haug, 1972; Myklestad, 1974) and diatom natural populations (Haug et al., 1973) under nutrient depleted conditions. In this connection, it is interesting that up to 60% of the ^{14}C was incorporated into LMWM in 6B, 6C and 6D microcosms at the end of the incubation (Table 6), concurring with the lowest nitrate levels measured in all experimental microcosms (Table 2). High relative incorporation of ^{14}C into LMWM has been frequently associated with growth limitation, as a result of the reduction of macromolecular synthesis rates and the derived accumulation of metabolic precursors (Morris et al., 1974; Morris & Skea, 1978; Li & Harrison 1982; Madariaga & Fernández, 1990)

The relationship between the physiological responses of phytoplankton and the simulated upwelling velocity depicted a consistent pattern. In general, the most marked increases in Chl *a* concentration, P^Bmax, and macromolecular SSR were measured in C and D microcosms, where higher upwelling velocities had been simulated. Moreover, differences in the relative incorporation of carbon into proteins and the P:C compositional ratio proved to be dependent on the rate of increasing irradiance. These findings indicate that sub-surface phytoplankton populations have the ability to adjust their physiological state, showing higher growth rates, different patterns of photosynthetic carbon metabolism and, as a consequence, modifying the cellular biochemical composition, in response to a range of upwelling regimes.

Sea-truth observations carried out during an advective pulse (cruise 4) indicated that phytoplankton populations exhibited a series of physiological changes similar to those measured in the experimental microcosms under high irradiance and nutrient-rich conditions. Although integrated Chl *a* concentration did not show a large increase, integrated carbon incorporation displayed a 3-fold increase compared to carbon incorporation averaged over during the stratification period. Similarly, parallel increases in the protein-C:carbohydrate-C ratio (Fig. 1) and the macromolecular SSR (Fig. 3) were measured. Protein SSR reached values above 1 day^{-1}, which agrees with field observations in other upwelling areas (Barlow, 1980), and during diatom blooms (Hitchcock, 1978; Hama et al., 1988; Fernández et al., 1992).

The similarity in patterns of macromolecular synthesis and biochemical composition of microalgae under simulated upwelling conditions in the laboratory and during an in situ upwelling pulse, indicates that irradiance and nutrient concentration are significant factors regulating the physiological state of phytoplankton in upwelling systems. Furthermore, the specific synthesis ratio of protein to storage products has been found to vary as a function of the increasing irradiance and, as a consequence, the P:C ratio of particulate matter becomes modified depending on the nature of the upwelling event. The changes in the biochemical composition of phytoplankton induced by the physical variability of upwelling, would reflect variations in the carbon to nitrogen uptake

ratio of phytoplankton, and therefore have a direct influence upon processes of a wide ecological significance such as the rate of CO_2 removal from the water (Laws, 1991), zooplankton ingestion and assimilation rates (Scott, 1980; Libourel-Houde & Roman, 1987) and the rate of mineralization of particulate matter (see Goldman et al., 1987). In consequence, our results demonstrate the significance of small scale variability of physico-chemical parameters in understanding the cycling of carbon within the planktonic compartment in upwelling systems.

Acknowledgements

This study was supported by grant number MAR88-0408 from the Spanish C.I.C.Y.T. J.A. Sostres provided nutrient analysis and R. González-Quirós and J.L. Acuña kindly helped with sampling routines. We also thank F.G. Figueiras, I. de Madariaga and two anonymous referees for their critical comments to a previous version of the manuscript. E.M. acknowledges the receipt of a PFPI fellowship from the Spanish Ministry of Science and Education.

References

Barlow, R.G., 1980. The biochemical composition of phytoplankton in an upwelling region off South Africa. *J. Exp. Mar. Biol. Ecol.*, Vol. 45, pp. 83–93.

Barlow, R.G., 1984. Physical responses of phytoplankton to turbulent and stable environments in an upwelling region. *J. Plankton Res.*, Vol. 6, pp. 385–397.

Cuhel, R.L., P.B. Ortner & D.R.S. Lean, 1984. Night synthesis of protein by algae. *Limnol. Oceanogr.*, Vol. 31, pp. 1364–1373.

Di Tullio, G.R. & E.A. Laws, 1983. Estimates of phytoplankton N uptake based on $^{14}CO_2$ incorporation into protein. *Limnol. Oceanogr.*, Vol. 28, pp. 177–185.

Dortch, Q. & T.T. Packard, 1989. Differences in biomass structure between oligotrophic and eutrophic marine ecosystems. *Deep-Sea Res.*, Vol. 36, pp. 223–240.

Dubois, M., K.A. Gilles, J.K. Hamilton, P.A. Rebers & F. Smith, 1956. Colorimetric method for determination of sugars and related substances. *Anal. Chem.*, Vol. 28, pp. 350–356.

Fernández, E., P. Serret, I de Madariaga, A.G. Davies & D.S. Harbour, 1992. Photosynthetic carbon metabolism and biochemical composition of spring phytoplankton assemblages enclosed in microcosms: the diatom-*Phaeocystis* sp. succession. *Mar. Ecol. Prog. Ser.*, Vol. 90, pp. 89–102.

Figueiras, F.G., K.J. Jones, A.M. Mosquera, X.A. Alvarez-Salgado, A. Edwards & N. MacDougall, 1994. Red tide assemblage formation in an estuarine upwelling ecosystem: Ria de Vigo. *J. Plankton Res.*, Vol. 16, pp. 857–878.

Goldman, J.C., D.A. Caron & M.R. Dennett, 1987. Regulation of gross growth efficiency and ammonium regeneration in bacteria by substrate C:N ratio. *Limnol. Oceanogr.*, Vol. 32, pp. 1239–1252.

Grasshoff, K., M. Ehrhardt & M. Kremling, 1983. *Methods of seawater analysis*. Verlag Chemie, Weinheim, second edition, 419 pp.

Hama, T.N., N. Handa, M. Takahashi, F. Whitney & C.S. Wong, 1988. Change in distribution patterns of photosynthetically incorporated C during phytoplankton bloom in controlled experimental ecosystem. *J. Exp. Mar. Biol. Ecol.*, Vol. 120, pp. 39–56.

Haug, A., S. Myklestad & E. Sakshaug, 1973. Studies on the ecology of the Trondheimsfjord. I. The chemical composition of phytoplankton populations. *J. Exp. Mar. Biol. Ecol.*, Vol. 11, pp. 15–26.

Hawes, I., 1990. The effects of light and temperature on photosynthate partitioning in Antarctic freshwater phytoplankton. *J. Plankton Res.*, Vol. 12, pp. 513–518.

Hitchcock, G.L., 1978. Labelling patterns of carbon-14 in net plankton during a winter-spring bloom. *J. Exp. Mar. Biol. Ecol.*, Vol. 69, pp. 21–36.

Hitchcock, G.L., 1983. Photosynthate partitioning in cultured marine phytoplankton. I. Dinoflagellates. *J. Exp. Mar. Biol. Ecol.*, Vol. 69, pp. 21–36.

Ishizaka, J., M. Takahashi & S. Ichimura, 1983. Evaluation of coastal upwelling effects on phytoplankton growth by simulated culture experiments. *Mar. Biol.*, Vol. 76, pp. 271–278.

Jason Smith, G., R.C. Zimmerman & R.S. Alberte, 1992. Molecular and physiological responses of diatoms to variable levels of irradiance and nutrient availability: growth of *Skelotonema costatum* in simulated upwelling conditions. *Limnol. Oceanogr.*, Vol. 37, pp. 989–1007.

Konopka, A. & M. Schnur, 1981. Effect of light intensity on macromolecular synthesis in cyanobacteria. *Microb. Ecol.*, Vol. 6, pp. 291–301.

Lancelot, C., S. Mathot & N.J.P. Owens, 1986. Modelling protein synthesis, a step to an accurate estimate of net primary production: *Phaeocystis pouchetii* colonies in Belgian coastal waters. *Mar. Ecol. Prog. Ser.*, Vol. 32, pp. 239–248.

Laws, E.A., 1991. Photosynthetic quotients, new production and net community production in the open ocean. *Deep-Sea Res.*, Vol. 38, pp. 143–167.

Lean, R.S. & B.K. Burnison, 1979. An evaluation of errors in the ^{14}C method of primary production measurement. *Limnol. Oceanogr.*, Vol. 24, pp. 917–928.

Li, W.K.W. & W.G. Harrison, 1982. Carbon flow into end-products of photosynthesis in short and long incubations of a natural phytoplankton population. *Mar. Biol.*, Vol. 72, pp. 175–182.

Li, W.K.W., H.E. Glover & I. Morris, 1980. Phisiology of carbon photoassimilation by *Oscillatoria thiebautii* in the Caribbean Sea. *Limnol. Oceanogr.*, Vol. 25, pp. 447–456.

Libourel-Houde, S.E. & M.R. Roman, 1987. Effects of food quality on the functional ingestion response of the copepod *Acartia tonsa*. *Mar. Ecol. Prog. Ser.*, Vol. 40, pp. 69–77.

Lohrenz, S.E. & C.D. Taylor, 1987. Primary production of protein: I. Comparison of net cellular carbon and protein synthesis with ^{14}C-derived rate estimates in steady-state cultures of marine phytoplankton. *Mar. Ecol. Prog. Ser.*, Vol. 35, pp. 277–292.

Lowry, M., J. Rosebrough, A.L. Farr & J.R. Randall, 1951. Protein measurement with the Folin phenol reagent. *J. Biol. Chem.*, Vol. 193, pp. 265–280.

Madariaga, I. de & E. Fernández, 1990. Photosynthetic carbon metabolism of size-fractionated phytoplankton during an experimental bloom in marine microcosms. *J. Mar. Biol. Assoc. U.K.*, Vol. 70, pp. 531–543.

Mague, T.H., E. Friberg, D.J. Hughes & I. Morris, 1980. Extracellular release of carbon by marine phytoplankton; a physiological approach. *Limnol. Oceanogr.*, Vol. 25, pp. 262–279.

Morris, I., 1981. Photosynthetic products, physiological state and phytoplankton growth. *Can. Bull. Fish. Aquat. Sci.*, Vol. 210, pp. 83–102.

Morris, I. & W. Skea, 1978. Products of photosynthesis in natural populations of marine phytoplankton from the Gulf of Maine. *Mar. Biol.*, Vol. 47, pp. 303–312.

Morris, I., H.E. Glover & C.S. Yenstch, 1974. Products of photosynthesis by marine phytoplankton: the effect of environmental factors on the relative rates of protein synthesis. *Mar. Biol.*, Vol 27, pp. 1–9.

Morris, I., A.E. Smith & H.E. Glover, 1981. Products of photosynthesis in phytoplankton off the Orinoco River and in the Caribbean Sea. *Limnol. Oceanogr.*, Vol. 26, pp. 1034–1044.

Myklestad, S., 1974. Production of carbohydrates by marine planktonic diatoms. II. Influence of the N/P ratio in the growth medium on the assimilation ratio, growth rate, and production of cellular and extracellular carbohydrates by *Chaetoceros affinis* var. *willei* (Gram) Hustedt and *Skeletonema costatum* (Grev.) Cleve. *J. Exp. Mar. Biol. Ecol.*, Vol. 29, pp. 161–179.

Myklestad, S. & A. Haug, 1972. Production of carbohydrates by the marine diatom *Chaetoceros affinis* var. *willei* (Gran.) Hustedt. I. Effect of the concentration of nutrients in the culture medium. *J. Exp. Mar. Biol. Ecol.*, Vol. 9, pp. 125–136.

Pitcher, G.C., J.J. Bolton, P.C. Brown & L. Hutchings, 1993. The development of phytoplankton blooms in upwelled waters of the southern Benguela upwelling system as determined by microcosm experiments. *J. Exp. Mar. Biol. Ecol.*, Vol. 165, pp. 171–189.

Platt, T. & A. Jassby, 1976. The relationship between photosynthesis and light for natural assemblages of coastal marine phytoplankton. *J. Phycol.*, Vol. 12, pp. 421–430.

Platt, T., C.L. Gallegos & W.G. Harrison, 1980. Photoinhibition of photosynthesis in natural assemblages of marine phytoplankton. *J. Mar. Res.*, Vol. 38, pp. 687–701.

Priscu, J.C. & L.R. Priscu, 1984. Photosynthate partitioning by phytoplankton in a New Zealand coastal upwelling system. *Mar. Biol.*, Vol. 81, pp. 31–40.

Rivkin, R.B., 1989. Influence of irradiance and spectral quality on the carbon metabolism of phytoplankton. I. Photosynthesis, chemical composition and growth. *Mar. Ecol. Prog. Ser.*, Vol. 55, pp. 291–304.

Scott, J.M., 1980. Effect of growth rate of the food algae on the growth/ingestion efficiency of a marine herbivore. *J. Mar. Biol. Assoc. U.K.*, Vol. 60, pp. 681–702.

Smith, R.E.H., P. Clément & E.J. Head, 1990. Night metabolism of recent photosynthate by sea ice algae in the high Arctic. *Mar. Biol.*, Vol. 107, pp. 255–261.